J. Biochem. 2009;145(3)403–409
doi:10.1093/jb/mvn178

TTP at Ser^{245} Phosphorylation by AKT is Required for Binding to 14-3-3

Shigeki Chiba, Mie Tokuhara, Eugene Hayato Morita and Shunnosuke Abe*

Laboratory of Molecular Cell Physiology, Faculty of Agriculture, Ehime University, 3-Tarumi, Matsuyama, Ehime 7908566, Japan

Received September 17, 2008; accepted December 22, 2008; published online January 2, 2009

Transferrin receptor trafficking protein (TTP) is a key molecule for selective internalization of the transferrin receptor (Tf-R) through endocytic protein complexes. To identify the proteins that directly regulate TTP, we performed a yeast two-hybrid analysis and identified 14-3-3, which can modulate the activation state of target proteins. Subsequent analyses demonstrated that TTP directly binds to multiple 14-3-3 isotypes via its Ser^{245} residue (Ser^{246} in human) and that these proteins are associated at the plasma membrane. Ser^{245} was also found to be a substrate for AKT and the resulting Ser^{245} phosphorylation induced the TTP–14-3-3 interaction. Exposure to hydrogen peroxide rapidly enhanced this association in an ovarian cell line. These results suggest that TTP Ser^{245} is the principal target for the modulation of this protein via the AKT signalling cascade.

Key words: 14-3-3, AKT, phosphorylation, interaction.

Abbreviations: Eps15, epidermal growth factor receptor pathway substrate 15; NPF, Asn-Pro-Phe; Tf-R, transferrin receptor; Ap2, clathrin adaptor protein 2; SH3, Src homology 3; EGFR, Epidermal Growth Factor Receptor; LDLR, low density lipoprotein receptor; AKT1, v-akt murine thymoma viral oncogene homolog 1; GST, glutathione S-transferase; PKC, Protein kinase C; PKA, Protein kinase A; CLK2, CDC-like kinase 2; CAMK2G, Calcium/calmodulin-dependent protein kinase II gamma; BAD, Bcl-2-associated death promoter.

INTRODUCTION

Transferrin receptor trafficking protein (TTP, also known as SH3BP4) was originally identified as a binding protein for the Eps15 (epidermal growth factor receptor pathway substrate 15) homology domain (*1*) and a suppressed gene in macular corneal dystrophy (MCD) fibroblasts (*2*). This vertebrate-specific 962 amino-acid (aa) protein (110 kDa) possesses several conserved domains and motifs, including two types of SH3-binding domains, three Asn-Pro-Phe (NPF) motifs, and several putative clathrin endocytic protein-binding sites (*2*, *3*). According to a recent report, TTP has been defined as a principal factor in the regulation of transferrin receptor (Tf-R) internalization (*4*). Serum iron–transferrin conjugates bind to Tf-R on the cell surface and are internalized via clathrin endocytic complexes, supplying iron for use the transport of oxygen and cellular enzyme activation. TTP directly binds to Tf-R via its SH3-binding domain and specifically internalizes this receptor via the clathrin endocytic complexes, but not other receptors (EGFR, LDLR), in epithelial cells (*4*).

To further understand the intracellular regulation of TTP, it will be important to identify and characterize its interacting factors. TTP forms large protein–protein complexes, which include interactions with several proteins of the endocytic system, including dynamin, Eps15, clathrin and Ap2 (*4*). However, there are few reports pertaining to the molecular basis of the direct modulation of TTP binding and its functional roles. For the identification of additional proteins that directly interact TTP may provide important clues to understanding its regulation, we performed a yeast two-hybrid screen in our current study to detect partner proteins. These experiments identified multiple isotypes of 14-3-3 as direct TTP-interacting partners.

Members of the 14-3-3 protein family frequently function via the direct conformational alteration of their binding partners, resulting in changes in their molecular interactions, phosphorylation states, activity, stability and sub-cellular localization (*5*, *6*). Moreover, we report herein that TTP Ser^{245} is a specific 14-3-3-binding site which is phosphorylated by the serine/threonine kinase AKT and that this interaction is enhanced by oxidative stress. AKT is activated by several growth factors, hormones and a variety of cellular stressors. The actions of AKT in the cell are numerous and diverse, but all result in anti-apoptotic or proliferative effects (*7*). Here, we provide evidence supporting a molecular mechanism for the direct modulation of TTP through AKT activity.

MATERIALS AND METHODS

cDNA and Plasmid Constructs—A mouse TTP/SH3BP4 (NM_133816) cDNA was obtained from NIH/3T3 mRNA by RT–PCR. 14-3-3 cDNAs were obtained from prey clones of a two-hybrid library by PCR. TTP deletion and point-mutant clones were constructed using a KOD mutagenesis kit (Toyobo, Osaka, Japan). These cDNAs

*To whom correspondence should be addressed. Tel: +81-89-946-9853, Fax: +81-89-946-9853,
E-mail: mcblab@mcb.agr.ehime-u.ac.jp

were cloned into pBlueScriptII SK(−) (Stratagene, La Jolla, CA, USA) and verified by sequencing. To construct the various types of expression vectors, cDNAs were transferred into pGADT7, pGBKT7 (Clontech, Palo-Alto, CA, USA), pET42b (Novagen, Madison, WI, USA), pTNT (Promega, Madison, WI, USA), pIRESneo3x-StrepTagII-FLAG (Tag inserted pIRESneo3; Clontech), pCMV-GST-N, pCMV-HA-C1, and pCMV-FLAG-C1 (Tag replaced pEGFP-C1; Clontech) vectors, respectively.

Yeast Two-Hybrid Screening—Matchmaker Yeast Two-Hybrid System 3 (Clontech) was used for the screening of interaction partners according to the manufacturer's instructions. As the bait, a fragment of mouse TTP (aa 48–962) was used, and as the prey the Matchmaker mouse 7-day embryo cDNA library (Clontech) was used. These were sequentially transformed into AH109 strain and screened under high stringency conditions (SD/−Leu, −Trp, −His, −Ade, +X-α-gal) for 10 days.

Cells and Stable Transfection—CHO-K1 cell line and its sublines were maintained in Ham's F-12 (Nihon Pharmaceutical, Tokyo, Japan) supplemented with 10% fetal bovine serum (Invitrogen, Grand Island, NY, USA) at 37°C under 5% CO_2. Expression vectors were transfected into CHO-K1 cells using TransFast (Promega) according to the manufacturer's instructions. To establish cell lines stably expressing TTP (CHO-TTP), pIRESneo3x-TTP-StrepTagII-FLAG was transfected into CHO-K1 cells and cultured with 400 μg/ml of G418 (Nakarai Tesque, Kyoto, Japan) for 2 weeks. G418-resistant colonies were isolated by the penicillin-cup method. The protein expression levels in individual clones were determined by immunoblotting.

In Vitro *Protein Expression*—FLAG-tagged wild-type and truncated TTP and 14-3-3σ were expressed using the TNT SP6 Quick-Coupled Transcription/Translation System (Promega) with a Transcend Biotin-Lysyl-tRNA (Promega) according to the manufacturer's instructions. Expressed proteins were subjected to *in vitro* co-immunoprecipitation and were detected using streptavidin-alkaline phosphatase (GE Healthcare, Waukesha, WI, USA).

Indirect Immunofluorescence—Transfected cells were subjected to immunofluorescence as described previously (*8*). HA-tagged TTP and endogenous 14-3-3 were probed with the anti-HA (3F10, Roche Diagnostic, Basel, Switzerland) and anti-14-3-3 (H8, Santa Cruz Biotechnology, Santa Cruz, CA, USA) primary antibodies, followed by AlexaFluor488 goat anti-mouse and AlexaFluor594 goat anti-rat (Invitrogen) secondary antibodies, respectively. Images were obtained using a Microphoto-FXA fluorescence microscope (Nikon, Tokyo, Japan) and PenguinPro 600CLM (Pixera, San Jose, CA) with a ×60 oil immersion objective lens and appropriate filter sets (AlexaFluor488, excitation 470/40 nm, emission 535/50 nm; AlexaFluor594, excitation 560/40 nm, emission 630/60 nm).

Immunoprecipitation and Immunoblotting—Cells were lysed in lysis buffer (50 mM Tris–HCl (pH 7.5), 150 mM NaCl, 10% glycerol, 200× protease inhibitor cocktail-I (Sigma, St Louis, MO, USA), 100× phosphatase inhibitor (Nakarai), 0.5% Triton X-100) and then clarified by centrifugation at 20,000 × *g* for 5 min. The supernatant was precleared with CL-4B (Sigma) and then incubated with anti-FLAG(M2) affinity-gel (Sigma) at 4°C for 1–2 h. The bound proteins were batch-purified and eluted with 200 μg/ml 3× FLAG peptide (Sigma) in lysis buffer. Eluted proteins were separated in a 10% SDS–PAGE mini gel and then transferred to a PVDF membrane. Membranes were incubated sequentially with Blocking-One (Nakarai), anti-FLAG (M2) (Sigma) or anti-14-3-3 antibodies, and HRP-conjugated anti-mouse IgG (GE Healthcare) or alkaline phosphatase-conjugated anti-mouse IgG (Sigma). Bound proteins were visualized using an ECL reagent (GE Healthcare) and FluorMAX (Bio-Rad Corp., Hercules, CA, USA), or using BCIP/NBT colorimetric substrates (Nakarai). Levels of precipitated proteins were determined by densitometry using Multi-Gauge software (FujiFilm, Tokyo, Japan).

Modified Tandem Affinity Purification—Lysates from CHO-TTP and mock-transfected cells were clarified by centrifugation at 20,000 × *g* for 15 min. Each supernatant was loaded onto a StrepTactin Superflow column (IBA, Göttingen, Germany) and the columns were washed and bound proteins were eluted with 15 mM desthiobiotin (Sigma) in lysis buffer. The eluted fractions were subjected to immunoprecipitation using an anti-FLAG affinity gel as described above. Purified proteins were separated in a 12% SDS–PAGE large gel and visualized with a Negative Stain kit (Nakarai). Several protein bands were excised from the gel and subjected to the LC–MS/MS at the UVIC genome BC proteomics centre.

In Vitro *Phosphorylation and GST Pulldowns*—A TTP fragment (aa 215–263), a mutant TTP fragment (aa 215–263, S245A) and a BCL2-antagonist of cell death (BAD, NM_007522) were inserted into the bacterial expression vector pET42b and introduced into BL21(DE3) cells. Cells were cultured to an OD_{600} of 0.7, and then GST-fusion protein expression was induced with 0.3 mM IPTG for 3 h at 30°C. Proteins were purified using Glutathione sepharose 4B Columns (GE Healthcare). GST-fusion proteins immobilized on sepharose columns were phosphorylated with 2 ng/μl of activated AKT1 (Upstate Biotechnology, Lake Placid, NY, USA) at 30°C for 15 min in kinase reaction buffer (20 mM MOPS–NaOH (pH 7.4), 15 mM $MgCl_2$, 1 mM EGTA, 0.2 mM dithiothreitol, 10 mM β-glycerol-phosphate, 10 mM NaF, 0.2 mM $NaVO_4$, 0.01% Brij-35, 100 μM ATP). CHO-K1 cell lysates were loaded onto the columns of immobilized phosphorylated proteins. The bound proteins were batch-purified, eluted with 20 mM reduced glutathione, and then purified by methanol chloroform extraction.

Fluorescence Detection of Phosphorylated and Total Protein—Electrophoresis gels were fixed and stained with ProQ diamond phosphoprotein stain (Invitrogen) followed by Flamingo total protein stain (Bio-Rad) according to the manufacturers' instructions. After each staining procedure, a gel image was obtained using FLA-3000G (FujiFilm) with an excitation 532 nm, and emission 580 nm long-path filter sets.

RESULTS AND DISCUSSION

Identification of 14-3-3 Isotypes as Directly TTP Interacting Proteins—To identify TTP-interacting partners, we performed yeast two-hybrid analysis. 4.1×10^6

independent transformants were screened and 228 positive clones were obtained under high stringency conditions. False positives and overlapping clones were excluded, and 23 positive clones were finally selected. These clones included Eps15 and dynamin as previously reported (*1*, *4*) as well as five isotypes of 14-3-3 (β, ε, ζ, η and θ). 14-3-3 is an accessory protein that modifies the function or activity of its binding partners. Thus, we selected 14-3-3 as a primary candidate for functioning as TTP regulators. Since the mammalian 14-3-3 protein family is comprised of seven highly conserved isotypes, we investigated potential TTP interactions with all 14-3-3 isotypes by spotting the co-transformants onto selection plates. Yeast spots grew only in the co-transformants consisting of TTP and any one of the 14-3-3 isotypes, but not in single transformants of TTP or 14-3-3 under high stringency conditions (Fig. 1A). These results indicate that all isotypes of 14-3-3 are potential candidates for directly binding to TTP.

To confirm these interactions, we established a CHO-K1 subline (CHO-TTP) which stably expresses double affinity-tagged-TTP and then isolated TTP protein complexes from these cells using modified-tandem affinity purification. These complexes were separated by electrophoresis and several protein bands were observed in the gel, with 28–31 kDa bands appearing especially clear and broad (Fig. 1B). These proteins were analysed by LC–MS/MS and subsequently identified as endogenous 14-3-3 isotypes including β, ε, γ, η, θ and ζ (Supplementary Fig. S1). These results further demonstrated the interaction of TTP and 14-3-3 and confirmed that multiple 14-3-3 isotypes are major components of the TTP protein complex. These data are also consistent with the results of a previous high throughput mass-spectrometric study of the 14-3-3σ protein complex (*9*).

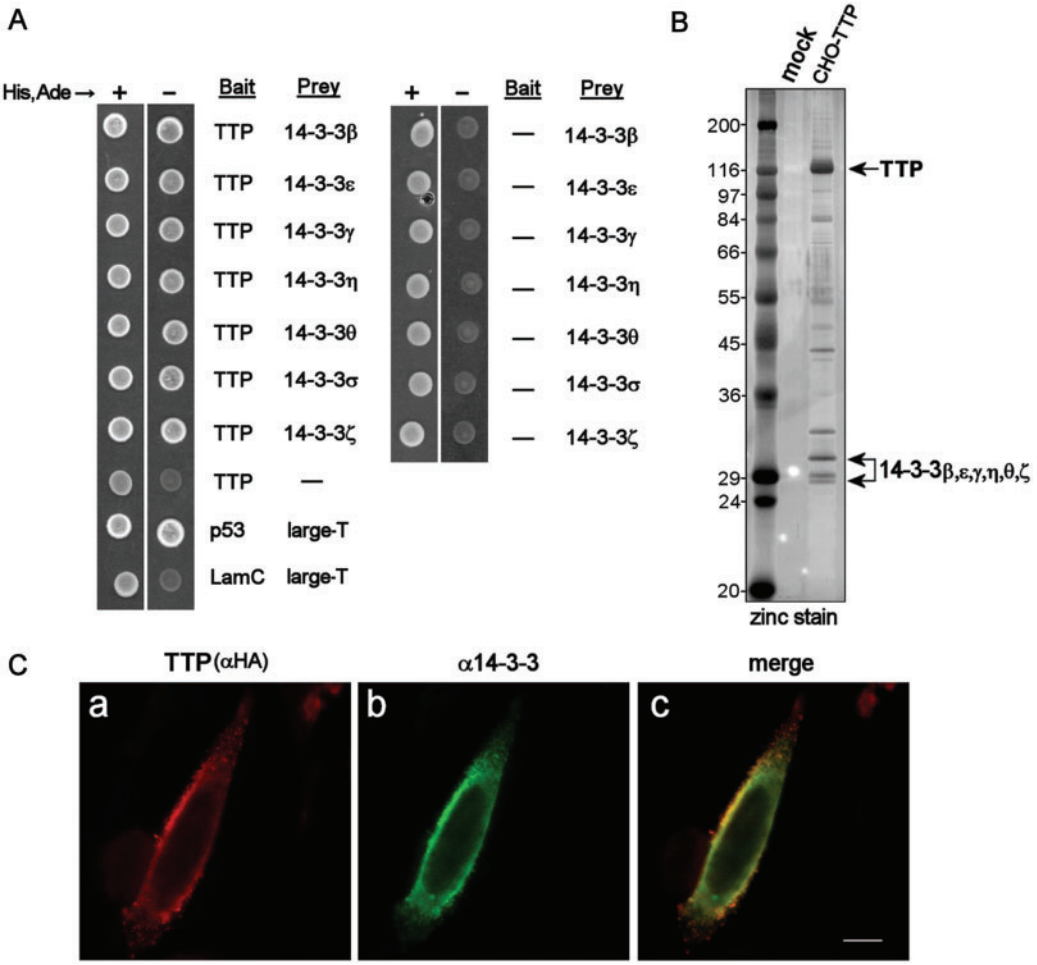

Fig. 1. **TTP interacts with multiple 14-3-3 isotypes.** (A) TTP interacts with seven 14-3-3 isotypes in a two-hybrid assay. Co-transformants were spotted onto low-stringency (+, −Leu, −Trp) or high-stringency (−, −His, −Ade, −Leu, −Trp) medium plates. The combinations of bait and prey plasmids are indicated on the right side of each panel. Large-T and LamC were used as a negative control, and large-T and p53 as a positive control. Bars represent the empty vector. (B) Multiple 14-3-3 isotypes were detected in the TTP–protein complex. TTP-interacting proteins were obtained by modified TAP using CHO-TTP (right lane) and mock (left lane) cells. Protein fragments of ~30 kDa (arrows) were identified by LC–MS/MS. (C) TTP and 14-3-3 co-localize at the periphery of the plasma membrane in CHO-K1 cells. TTP-HA was expressed in CHO-K1 cells and detected with an anti-HA primary antibody followed by an Alexa594-labelled anti-rat secondary antibody (a). Endogenous 14-3-3 proteins were detected with an anti-14-3-3 primary antibody followed by an Alexa488-labelled anti-mouse secondary antibody (b). Merged images are shown in (c). Bars, 10 μm.

TTP is reported to be localized at the plasma membrane, endocytic-vesicles and the nucleus (*3*, *4*), whereas 14-3-3 is localized at the plasma membrane, cytoplasm and nucleus (*10*). We next examined the intracellular co-localization of TTP and 14-3-3 proteins in CHO-K1 cells by immunofluorescence (Fig. 1C). Overlapping patterns of TTP and 14-3-3 staining were observed mainly at the periphery of the plasma membrane (Fig. 1C), but few or no endocytic vesicles and nucleus were observed to overlap (data not shown). These observations suggest that the association of TTP and 14-3-3 occurs at the periphery of the plasma membrane.

Identification of the 14-3-3-Binding Site on TTP—Generally, 14-3-3 acts as a regulator of target proteins by masking specific sequences of target proteins through their 14-3-3-binding domain (*11*). To map the 14-3-3-binding sites on TTP, we performed co-immunoprecipitations using *in vitro*-expressed 14-3-3 and various deletion fragments of TTP. The binding of 14-3-3 to TTP was observed with the aa 230–962 fragment, but not with the aa 257–962 fragment (Fig. 2B). These results indicated that the 14-3-3-binding site is in the aa 230–257 region on TTP. Interestingly, this region of TTP is widely and perfectly conserved among different classes of vertebrates (Fig. 2C). To predict the 14-3-3-binding domain recognition sites on TTP, a Scansite search was performed using the 14-3-3 mode1 profile. This program identifies protein interaction or phosphorylation sequence motifs using motif profile-scoring algorithms (*12*). Four putative recognition sites on TTP were identified (sequence, scoring percentiles): Ser^{19} (LPRCKS*EG, 0.191%), Thr^{118} (NYRNS*TLS, 0.655%), Ser^{245} (RSKRSYS*LS, 0.099%), and Ser^{372} (NSDRSTS*VS, 0.447%). Among these predicted sites, the score for Ser^{245} was significantly higher (a lower scoring percentile) than scores for the other potential sites. Ser^{245} is located within the aa 230–257

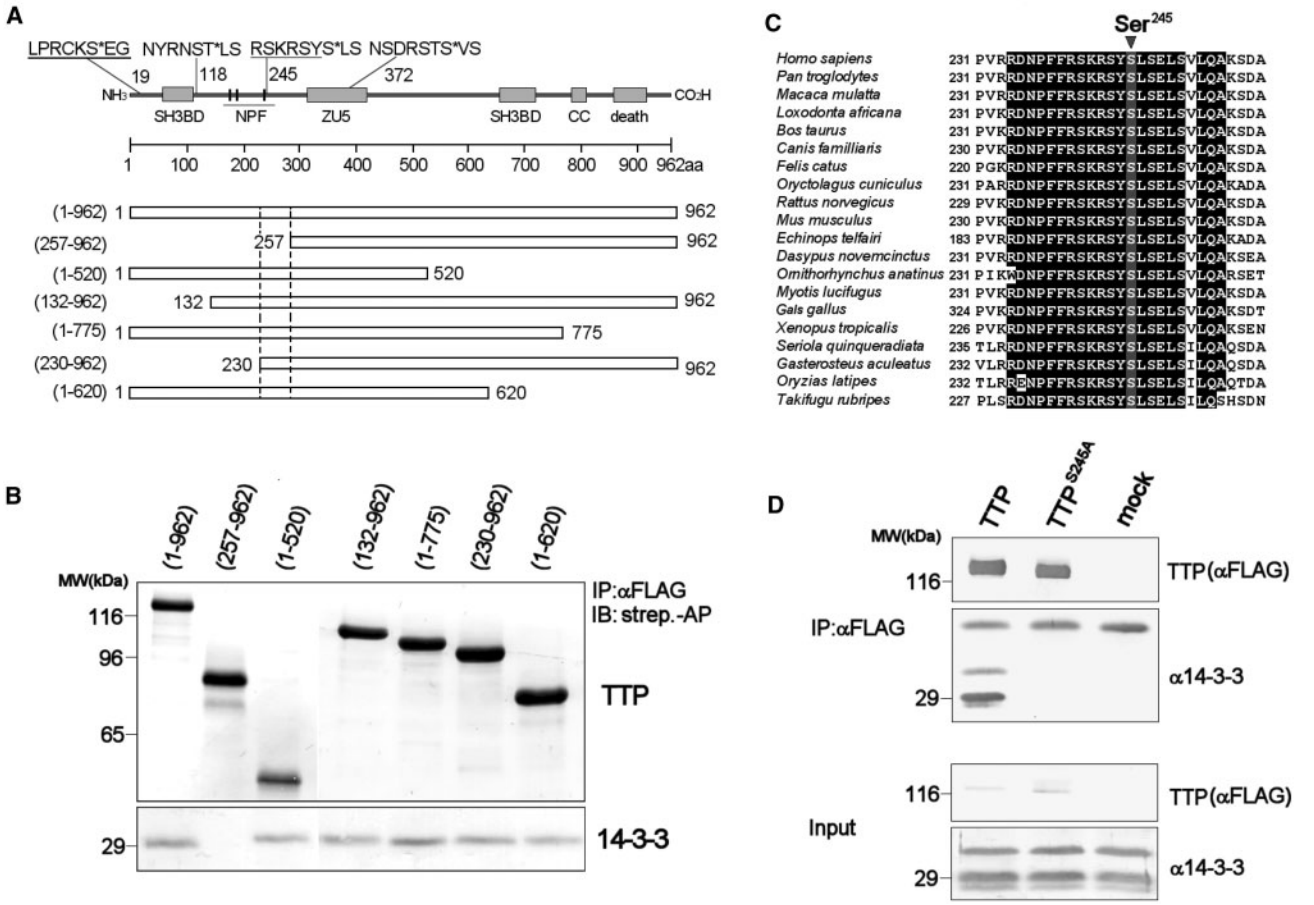

Fig. 2. **14-3-3 proteins directly bind to Ser^{245} of TTP.** (A) Four putative 14-3-3-binding sites were predicted by Scansite. Site positions and sequences are depicted in the diagram shown for mouse TTP (top picture). Amino-acid positions are indicated by the scale in the lower diagram, indicating the location of each deletion fragment in (B). (B) The aa 230–257 region contains a 14-3-3-binding site. *In vitro*-expressed 14-3-3σ (lower panel) and FLAG-tagged TTP fragments (upper panel) were subjected to co-immunoprecipitation with anti-FLAG affinity gel. Proteins were probed with streptavidin-alkaline phosphatase. (C) The flanking sequence of Ser^{245} is well conserved among numerous vertebrate species. The aa 230–257 region in mouse TTP was compared with homologous regions of TTP in different classes of vertebrates using ClustalW. The inverted regions show more than 19 matches in the 20 sequences aligned. (D) 14-3-3 binds to Ser^{245} on TTP. TTP-FLAG, TTP^{S245A}-FLAG or FLAG only (mock) were expressed in CHO-K1 cells and then subjected to immunoprecipitation using anti-FLAG affinity-gel (IP) with detection by immunoblotting with anti-FLAG M2 (top panel) and anti-14-3-3 H8 (second panel) antibodies. This 14-3-3 antibody recognizes all seven isotypes of this protein. The total precipitated-proteins from the same amount of extracts (Input) were loaded into each lane. The bands at the 38 kDa position which are present in all of the lanes are non-specific.

region and the Ser^{245} site, R-S-K-R-S-Y-S*-L-S is similar to the optimal 14-3-3 recognition motif, R-S-X-S*/T*-X-P. Although the Ser^{245} site lacked the final 'P', this aa is not essential for binding to 14-3-3 as with Ser^{642} in Wee1 and Ser^{359} in PTPH1 (*13*, *14*). Thus, Ser^{245} was the best potential candidate site on TTP for 14-3-3 binding.

To confirm this possibility, we generated a TTP point mutant in which Ser^{245} was converted to Ala^{245} (TTP^{S245A}) and performed co-immunoprecipitation analyses in CHO-K1 cells. Endogenous 14-3-3 proteins were indeed found to be co-precipitated with wild-type TTP, but not with TTP^{S245A} (Fig. 2D). Meanwhile, mutants of other potential sites via alanine substitutions: TTP^{S19A}, TTP^{T118A}, TTP^{S372A} still interacted with 14-3-3 proteins as efficiently as wild-type TTP (Supplementary Fig. S2). These results demonstrate that 14-3-3 proteins directly bind to TTP Ser^{245} and that this site is essential for this association.

TTP at Ser^{245} is a Novel Substrate of AKT Kinase— 14-3-3 typically binds to phosphorylated Ser/Thr-containing motifs, although phosphorylation-independent interactions have also been previously observed (*15*). To examine whether TTP Ser^{245} could undergo phosphorylation, truncated TTP and TTP^{S245A} were expressed in CHO-K1 cells and the phosphorylation status of Ser^{245} was determined using the ProQ diamond phosphoprotein stain. The signal strength of this reagent correlates with the number of phosphorylated residues, with three orders of linear dynamic range. Phosphorylation was detected on TTP but not on TTP^{S245A} (Fig. 3A),

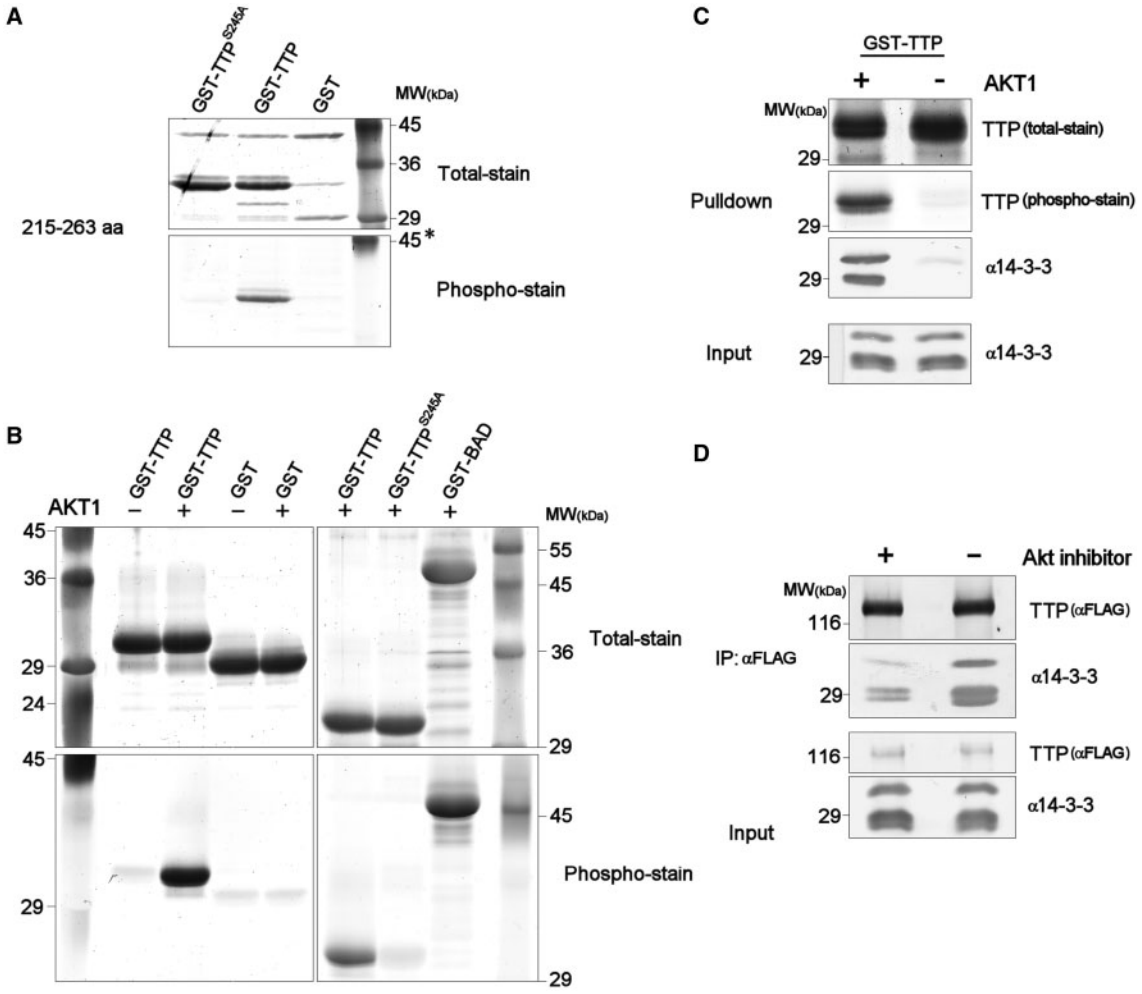

Fig. 3. **Ser^{245} on TTP was directly phosphorylated by AKT1.** (A) A TTP fragment is phosphorylated at Ser^{245} in CHO-K1 cells. GST-TTP$_{(215–263)}$, GST-TTP$^{S245A}{}_{(215–263)}$ and GST were expressed in CHO-K1 cells and subjected to GST pulldown. Phosphorylation status were then examined using ProQ-diamond phosphoprotein stain (lower panel), followed by Flamingo total protein stain (upper panel). The 45-kDa molecular weight marker represents phosphorylated ovalbumin. (B) The Ser^{245} residue of TTP is directly phosphorylated by AKT1. Bacterially expressed GST-TTP$_{(215–263)}$, (GST-TTP), GST-TTP$^{S245A}{}_{(200–280)}$, (GST-TTP^{S245A}), GST-Bad and GST alone were incubated with (+) or without (–) activated AKT1 kinase. Protein phosphorylation was then examined as described above. (C) 14-3-3 binds to phosphorylated Ser^{245}. CHO-K1 cell lysates were subjected to GST pulldown using AKT-phosphorylated (+) or unphosphorylated (–) GST-TTP$_{(215–263)}$. The phosphorylation status of the purified proteins was examined as described above (top and second panels), followed by immunoblotting with anti-14-3-3 antibody (third panel). (D) An AKT inhibitor prevents the binding of 14-3-3 to TTP. CHO-TTP cells were treated with (+) or without (–) 15 μM AKT inhibitor VIII for 4 h and then subjected to immunoprecipitation using anti-FLAG affinity-gel. Proteins were detected by immunoblotting with anti-FLAG (top panel) and anti-14-3-3 (second panel) antibodies.

suggesting that Ser^{245} is a potent phosphorylation site. In order to identify the kinase responsible for Ser^{245} phosphorylation, a Scansite search was performed using full kinase profiles. Four putative Ser^{245} kinases were identified (scoring percentile): AKT (0.151%), PKCε (0.666%), Clk2 (0.466%) and CAMK2G (0.436%). The score for AKT was significantly higher than that of the other kinases. Although the typical AKT phosphorylation motif is R-X-R-X-X-S/T* (*, phosphorylation) (*16*), another phosphorylation motif, R-R/S/T-X-S*-X-S/T, has recently been described (*17*) as with Ser^{642} in Wee1 (*13*). Significantly, this alternative motif matches the TTP Ser^{245} site, RSK-R-S-Y-S*-L-S.

To examine whether the AKT kinase could directly phosphorylate the TTP Ser^{245} residue, we performed *in vitro* phosphorylation assays using several GST (glutathione-S-transferase)-fused protein fragments. GST-BAD (positive control) and GST-TTP$_{(215–263)}$ were heavily phosphorylated by activated AKT1, but GST-TTP$^{S245A}_{(215–263)}$ and GST alone were not phosphorylated (Fig. 3B). To next determine whether the 14-3-3 binding to TTP was phosphorylation-dependent, we performed a phosphorylation-mediated GST pulldown (Fig. 3C) and indeed found that 14-3-3 only binds to TTP that had been phosphorylated.

To confirm whether these *in vitro* results would also be observed *in vivo*, we assessed Ser^{245} phosphorylation using a typical AKT-substrate antibody in the presence or absence of an AKT inhibitor in CHO-TTP cells. However, no phosphorylation signal was detected (data not shown). As an alternative approach, we determined the Ser^{245} phosphorylation status indirectly by examining the rate of 14-3-3 binding to TTP using AKT inhibitor VIII. This inhibitor specifically and directly inhibits both the activation of AKT as well as its kinase activity, but does not affect the AGC family kinases. The levels of co-precipitated 14-3-3–TTP complexes were decreased by ~65% in the presence of AKT inhibitor VIII (Fig. 3D). These results show that TTP Ser^{245} is a AKT kinase substrate. This is the first identification of a specific kinase phosphorylating TTP.

AKT is a well-established downstream target of PI-3K (phosphatidylinositol 3-kinase) and PDK1/2 (pyruvate dehydrogenase kinase) signalling. It is activated by various growth factors and hormones, including insulin, EGF, VGF and PDGF; and by various cellular stresses, including heat, hypoxia and oxidation (*7*). AKT has critical roles in the activation of proliferation signalling cascades and in protecting the cell against apoptotic pathways involving BAD, BAX, caspase-9 and p53 (*18*). Hence, the AKT-dependent phosphorylation of TTP may elicit a positive effect on cell growth and the maintenance of cell viability.

It is important to note that AKT is one of the kinase that phosphorylates TTP on Ser^{245}, and that it is possible that other kinases such as PKA and CAMK2G might also regulate TTP via Ser^{245} phosphorylation. This possibility remains to be investigated.

14-3-3-Binding Rate to TTP is Increased Upon H2O2 Exposure—It has been proposed previously that TTP is a target of oxidative stress response pathways in RPE cells (*3*, *19*, *20*), and the Tf-R internalization event is critically affected by the oxidative stress response in some cell lines (*21–24*). In various cell lines also, AKT has been reported to be rapidly activated by several oxidant species to protect the cells from oxidative stress (*24–26*).

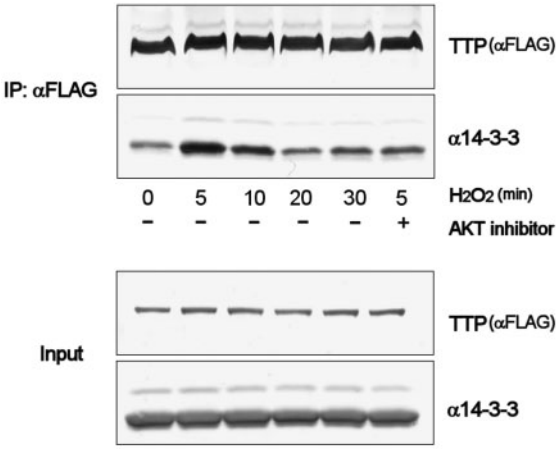

Fig. 4. **H_2O_2 rapidly enhances the binding of 14-3-3 to TTP.** CHO-TTP cells were serum-starved, pre-treated with (+) or without (–) 15 μM AKT inhibitor VIII for 30 min, and exposed to 400 μM H_2O_2 for 0–30 min, followed by immunoprecipitation using anti-FLAG affinity-gel (IP). Precipitated-proteins were analysed by immunoblotting with anti-FLAG (top panel) and anti-14-3-3 (second panel) antibodies.

To elucidate the upstream signalling events that initiate Ser^{245} phosphorylation, we examined the 14-3-3-binding rate following hydrogen peroxide (H_2O_2) exposure to induce oxidative stress in CHO-TTP cells. The-binding rate of 14-3-3 to TTP immediately increased upon H_2O_2 exposure and reached a peak of ~3.2-fold after 5 min (Fig. 4). This increased binding was inhibited by AKT inhibitor VIII (right-hand lane). These results indicated that H_2O_2 induced TTP phosphorylation by AKT and promotes 14-3-3 association with TTP. These findings suggest that one of the upstream signalling cascades that initiates the TTP and 14-3-3 association is the cellular response to oxidative stress.

In our present study, we have further elucidated the molecular interactions and modification events associated with TTP. In summary, TTP Ser^{245} is a novel AKT substrate and that phosphorylation of Ser^{245} induces multi-isotypes of 14-3-3 associations with TTP at the periphery of the plasma membrane. In addition, one upstream initiator of this interaction is the oxidative stress response. These molecular-based analyses contribute to the current understanding of the intracellular role of TTP, and suggest a possible linkage between AKT-mediated survival cascades and the transferrin-internalizing event.

SUPPLEMENTARY DATA

Supplementary data are available at *JB* online.

ACKNOWLEDGEMENTS

We thank the RIKEN BioResource Center for providing mammalian cell lines. We also thank the Integrated Center

for Science, Ehime University, for technical support and the use of equipment. Special thanks to Prof. Ikuya Sakai and Prof. Eric Davis for their critical proofreading of this manuscript.

CONFLICT OF INTEREST

None declared.

REFERENCES

1. Salcini, A.E., Confalonieri, S., Doria, M., Santolini, E., Tassi, E., Minenkova, O., Cesareni, G., Pelicci, P.G., and Di Fiore, P.P. (1997) Binding specificity and in vivo targets of the EH domain, a novel protein-protein interaction module. *Genes Dev.* **11**, 2239–2249
2. Dunlevy, J.R., Berryhill, B.L., Vergnes, J.P., SundarRaj, N., and Hassell, J.R. (1999) Cloning, chromosomal localization, and characterization of cDNA from a novel gene, SH3BP4, expressed by human corneal fibroblasts. *Genomics* **62**, 519–524
3. Khanobdee, K., Kolberg, J.B., and Dunlevy, J.R. (2004) Nuclear and plasma membrane localization of SH3BP4 in retinal pigment epithelial cells. *Mol. Vis.* **10**, 933–942
4. Tosoni, D., Puri, C., Confalonieri, S., Salcini, A.E., De Camilli, P., Tacchetti, C., and Di Fiore, P.P. (2005) TTP specifically regulates the internalization of the transferrin receptor. *Cell* **123**, 875–888
5. Bridges, D. and Moorhead, G.B. (2005) 14-3-3 proteins: a number of functions for a numbered protein. *Sci. STKE* **2005**, re10
6. Fu, H., Subramanian, R.R., and Masters, S.C. (2000) 14-3-3 proteins: structure, function, and regulation. *Annu. Rev. Pharmacol. Toxicol.* **40**, 617–647
7. Brazil, D.P. and Hemmings, B.A. (2001) Ten years of protein kinase B signalling: a hard Akt to follow. *Trends Biochem. Sci.* **26**, 657–664
8. Benmerah, A., Poupon, V., Cerf-Bensussan, N., and Dautry-Varsat, A. (2000) Mapping of Eps15 domains involved in its targeting to clathrin-coated pits. *J. Biol. Chem.* **275**, 3288–3295
9. Benzinger, A., Muster, N., Koch, H.B., Yates, J.R. 3rd., and Hermeking, H. (2005) Targeted proteomic analysis of 14-3-3 sigma, a p53 effector commonly silenced in cancer. *Mol. Cell Proteomics* **4**, 785–795
10. Muslin, A.J. and Xing, H. (2000) 14-3-3 proteins: regulation of subcellular localization by molecular interference. *Cell Signal.* **12**, 703–709
11. Yaffe, M.B., Rittinger, K., Volinia, S., Caron, P.R., Aitken, A., Leffers, H., Gamblin, S.J., Smerdon, S.J., and Cantley, L.C. (1997) The structural basis for 14-3-3:phosphopeptide binding specificity. *Cell* **91**, 961–971
12. Obenauer, J.C., Cantley, L.C., and Yaffe, M.B. (2003) Scansite 2.0: Proteome-wide prediction of cell signaling interactions using short sequence motifs. *Nucleic Acids Res.* **31**, 3635–3641
13. Katayama, K., Fujita, N., and Tsuruo, T. (2005) Akt/protein kinase B-dependent phosphorylation and inactivation of WEE1Hu promote cell cycle progression at G2/M transition. *Mol. Cell Biol.* **25**, 5725–5737
14. Zhang, S.H., Kobayashi, R., Graves, P.R., Piwnica-Worms, H., and Tonks, N.K. (1997) Serine phosphorylation-dependent association of the band 4.1-related protein-tyrosine phosphatase PTPH1 with 14-3-3beta protein. *J. Biol. Chem.* **272**, 27281–27287
15. Masters, S.C., Pederson, K.J., Zhang, L., Barbieri, J.T., and Fu, H. (1999) Interaction of 14-3-3 with a nonphosphorylated protein ligand, exoenzyme S of Pseudomonas aeruginosa. *Biochemistry* **38**, 5216–5221
16. Obata, T., Yaffe, M.B., Leparc, G.G., Piro, E.T., Maegawa, H., Kashiwagi, A., Kikkawa, R., and Cantley, L.C. (2000) Peptide and protein library screening defines optimal substrate motifs for AKT/PKB. *J. Biol. Chem.* **275**, 36108–36115
17. Gnad, F., Ren, S., Cox, J., Olsen, J.V., Macek, B., Oroshi, M., and Mann, M. (2007) PHOSIDA (phosphorylation site database): management, structural and evolutionary investigation, and prediction of phosphosites. *Genome Biol.* **8**, R250
18. Manning, B.D. and Cantley, L.C. (2007) AKT/PKB signaling: navigating downstream. *Cell* **129**, 1261–1274
19. Khanobdee, K., Tesluk, L.A., Kolberg, J.B., and Dunlevy, J.R. (2003) The subcellular localization of SH3BP4 in human retinal pigment epithelial and cos-7 cell lines. *Invest. Ophthalmol. Vis. Sci.* **44**, 4544
20. Koppelman, E.D., Kolberg, J.B., and Dunlevy, J.R. (2003) Characterization of the novel protein SH3BP4 death domain during oxidant-induced apoptosis in human pigment epithelial (ARPE-19) cells. *Invest. Ophthalmol. Vis. Sci.* **44**, 4545
21. Cheng, J. and Vieira, A. (2006) Oxidative stress disrupts internalization and endocytic trafficking of transferrin in a human malignant keratinocyte line. *Cell Biochem. Biophys.* **45**, 177–184
22. Malorni, W., Testa, U., Rainaldi, G., Tritarelli, E., and Peschle, C. (1998) Oxidative stress leads to a rapid alteration of transferrin receptor intravesicular trafficking. *Exp. Cell Res.* **241**, 102–116
23. Kotamraju, S., Chitambar, C.R., Kalivendi, S.V., Joseph, J., and Kalyanaraman, B. (2002) Transferrin receptor-dependent iron uptake is responsible for doxorubicin-mediated apoptosis in endothelial cells: role of oxidant-induced iron signaling in apoptosis. *J. Biol. Chem.* **277**, 17179–17187
24. Tampo, Y., Kotamraju, S., Chitambar, C.R., Kalivendi, S.V., Keszler, A., Joseph, J., and Kalyanaraman, B. (2003) Oxidative stress-induced iron signaling is responsible for peroxide-dependent oxidation of dichlorodihydrofluorescein in endothelial cells: role of transferrin receptor-dependent iron uptake in apoptosis. *Circ. Res.* **92**, 56–63
25. Wang, X., McCullough, K.D., Franke, T.F., and Holbrook, N.J. (2000) Epidermal growth factor receptor-dependent Akt activation by oxidative stress enhances cell survival. *J. Biol. Chem.* **275**, 14624–14631
26. Mehdi, M.Z., Azar, Z.M., and Srivastava, A.K. (2007) Role of receptor and nonreceptor protein tyrosine kinases in H2O2-induced PKB and ERK1/2 signaling. *Cell Biochem. Biophys.* **47**, 1–10